

# ANALYSIS OF AIR POLLUTION IMAGE DATA

*P. Slavíková, M. Mudrová*

Institute of Chemical Technology, Faculty of Chemical Engineering

Department of Computing and Control Engineering

## Abstract

Air pollution is a global problem all over the world. Bioindicator approach is a modern and progressive way how to determinate an amount of damage caused by pollution in nature. Presented paper deals with processing of electron-microscope images of needles pores of Norway spruce. These needles have usually miscellaneous structure of epidermis. But if the tree grows in polluted air the needles start to cover by epicuticular waxes to protect themselves and stoma epidermis incrusts. Level of incrustation can be differentiated into five classes and it can solve as an indicator of level of air pollution. The goal of the work is a development of automatic algorithm which can recognize the level of stoma changes.

There are various accesses leading to a solution of the given problem of texture classification. Two principles discussed in our paper are based on the edge detection and wavelet analysis. By means of these methods, classification criteria were chosen and applied on a library of known samples of stoma texture to generate classification tables. Classification tables were tested on sets of unknown images of stoma in comparison with sensual classification. The best criterion was chosen for processing of the whole set of images taken from the various points in the Czech Republic.

## 1 Image Processing and Air Pollution

Study of needle epidermis texture is useful for air pollution monitoring as the epidermis is the first place of contact of tree with polluted air. For our research, the Norway spruce was chosen because of its large territory of occurrence.

Previous studies proved that structure properties of needle epidermis are dependent on degree of air pollution. If the tree grows in a clean air, the epidermis with stomas\* has miscellaneous structure. But when a quality of the air became worse, the needle epidermis starts to cover by epicuticular waxes to protect themselves against pollutants. For the air pollution quantification, five classes of epidermis coverage were defined and it specifies a pollution degree in dependence of epidermis damage. [1]

Table 1: CLASSES OF COVERING EPIDERMIS BY EPICUTICULAR WAXES IN DEPEND OF AIR POLLUTION

<i>Class</i>	<i>Description</i>
1	unaffected generous stoma wax with clearly visual funicle**, wax covering max. 10% from stoma area
2	count and size of the funicle is growing on different places of the stoma, creation of low area aggregates (wax "tuffs"), wax covering 10 - 25% from stoma area
3	often wax tuffs and a large area plates of waxes, wax covering 25 - 50% from stoma area
4	advanced degree of pollution damage, 50 – 75% of stoma area is covered by low area aggregates and large area wax plates
5	epistomal area is almost whole or whole covered by amorphous wax crust, more than 75% of stoma area is covered by large area wax plates

\* stoma (bot.) = part of needle/leaf epidermis which flower/tree use for breathing

\*\* funicle (bot.) = fibre

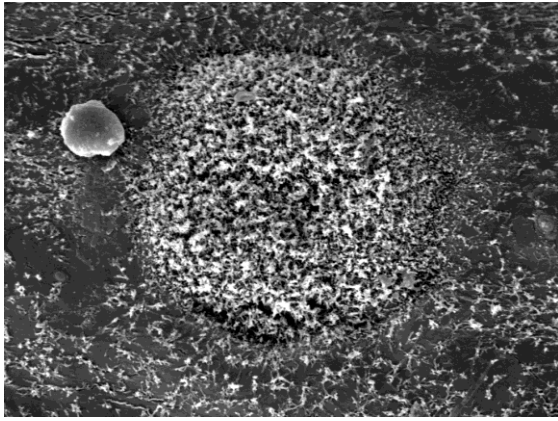


Figure 1: 1<sup>st</sup> class stoma

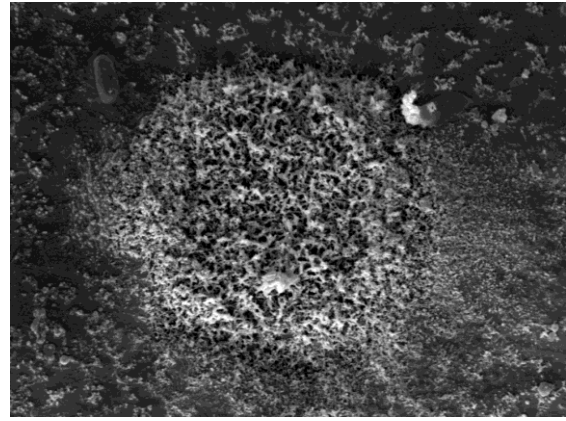


Figure 2: 2<sup>nd</sup> class stoma

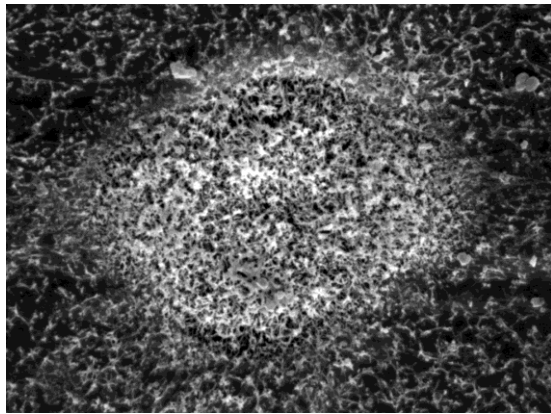


Figure 3: 3<sup>rd</sup> class stoma

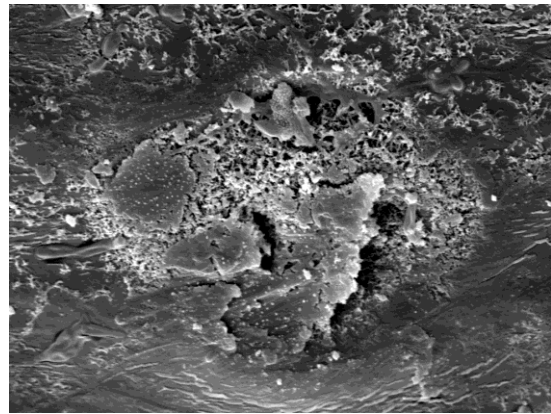


Figure 4: 4<sup>th</sup> class stoma

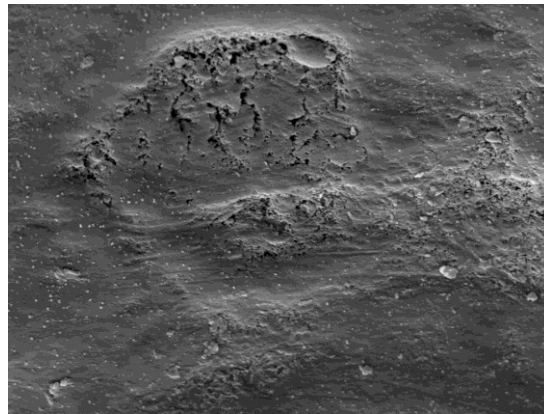


Figure 5: 5<sup>th</sup> class stoma

## 2 Mathematical Background

### 2.1 Edge Detection

Robinson, Prewitt, Kirsch and Sobel approach are simple methods for edge detection. Principle of these methods is intensity filter matrix which simulates fast brightness changes of the edge. There is not only one matrix but set of them when everyone detects edge in one direction. These matrices provides convolution masks. Canny algorithm is another commonly used method which exploits comparison of different resolution parameters and apply the best of them. [4]

## 2.2 Wavelet Transform in Image Processing

Discrete wavelet transform (1) is a mathematical method which uses wavelet and scaling function to signal decomposition. Wavelet and scaling functions are complementary filters and decompose signal into two frequency bands:

- *wavelet function* – high-pass filter
- *scaling function* – low-pass filter

$$DWT\{x(k)\} = X(m, n) = 2^{-\frac{m}{2}} \sum_k x(k) \psi(2^{-m}k - n) \quad (1)$$

Fig. 6 describes algorithm of wavelet decomposition. A signal  $x(n)$ , length  $N$ , is convolved with derived wavelet function  $\psi(n)$  at first and after that with corresponding scaling function  $\phi(n)$ . Output signal has approximately  $N$  wavelet coefficients  $q(n)$  and  $N$  scaling coefficients  $p(n)$ , so it is necessary to downsample output signal to its original length. Input sequence is decomposed into two frequency bands after the first level decomposition. Next step of the algorithm is a convolution of the first level scaling coefficients with derived wavelet and scaling function again and repeat downsampling.

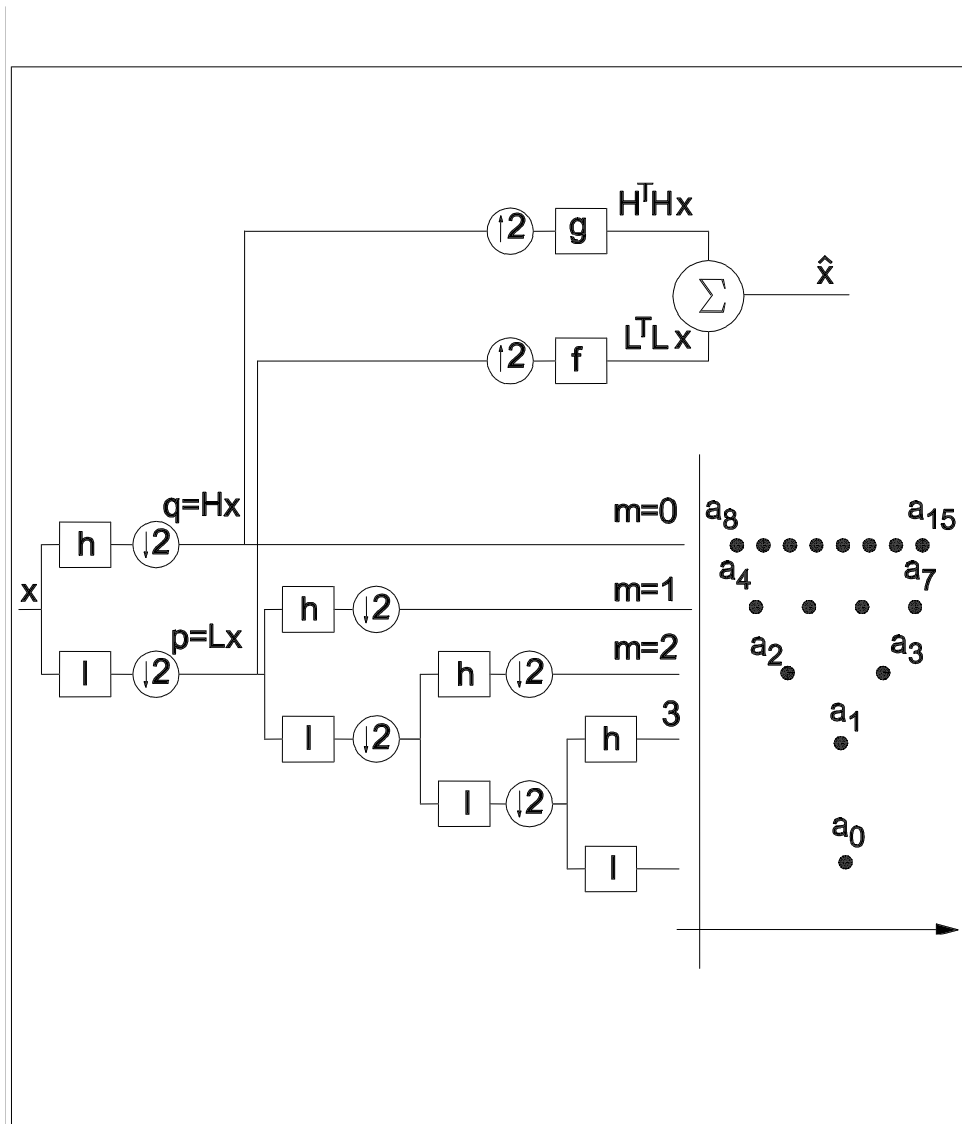


Figure 6: Wavelet decomposition of signal  $x(n)$

Wavelet decomposition of images is possible, as well. Distribution of wavelet and scaling coefficients is shown in Fig. 7.

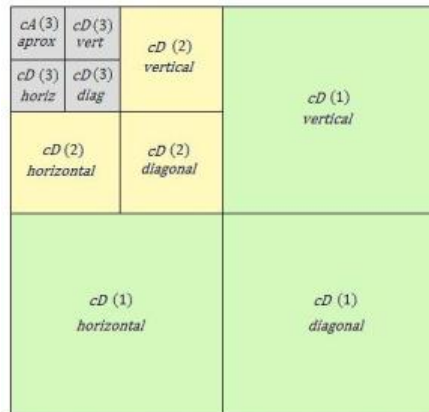


Figure 7: Image wavelet decomposition

### 3 Texture Classification

The first approach stoma images classification into 5 classes is based on the edge detection. A texture was classified by sum of pixels representing edges in the stoma image. A principle of classification is decreasing amount of detected edges with increasing degree of wax coverage. Classification table (Table 2) is used for comparison with wavelet classification criteria which are presented in this paper. More details about this method can be found in [2].

Table 2: CLASSIFICATION TABLE BASED ON EDGE DETECTION

Criterion	Class				
	1	2	3	4	5
$K_g$	> 2850	(2850;2650)	(2650;2300)	(2300;2000)	2000 >

The second principle based on wavelet transform is taking advantage of different energetic levels in images of each class of pollution in various levels of decomposition. Decreasing total energy of image is expected with increasing class of pollution. Low class images have miscellaneous structure which is represented by high energy gray-scale colours. At the opposite of this, high class images have coherent texture with dominant low-energy gray-scale colours.

The presumptions given above were verified on the set of 50 selected texture images (128 × 128 p) – a part of them is presented in Table 3.

#### 3.1 Image Pre-processing

Image comparison and development of classification algorithm is very essence of this work, so it is necessary to standardize images. Only after this procedure images results will be correct and reliable. Conversions to unified resolution, brightness and size were applied.

Last pre-processing method used for successful image classification was median filtering. The presence of white spots in images of the fifth class is the reason for using this type of pre-processing. These spots have high energy and influence low-energy level of fifth class images. Example of median filtering application to stoma image is shown in Table 4.

Table 3: EXAMPLE OF TEXTURE SAMPLES

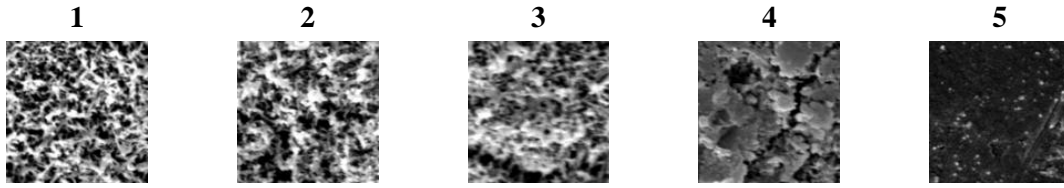
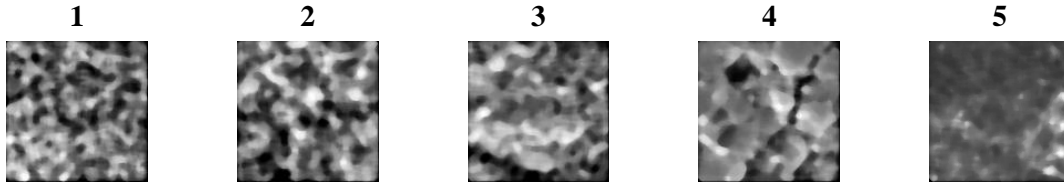


Table 4: EXAMPLE OF TEXTURE SAMPLES AFTER PRE-PROCESSING



### 3.2 Classification Criteria

Daubechies wavelet functions 1 – 10 were chosen for testing. Images of library were decomposed by means of all these functions and a sum of resulting wavelet coefficients was determined. Figures 8a, b show dependence of wavelet coefficients sum on a decomposition level. Basic requirement for classification criterion is a good separation of each image class. The best results were obtained by Daubechies 8 function (Fig. 8a) and sufficient results were provided by Daubechies 1 function, as well (Fig. 8b). According to these facts, classification criteria  $K_e$ ,  $K_{s1}$  and  $K_{s2}$  were determined.

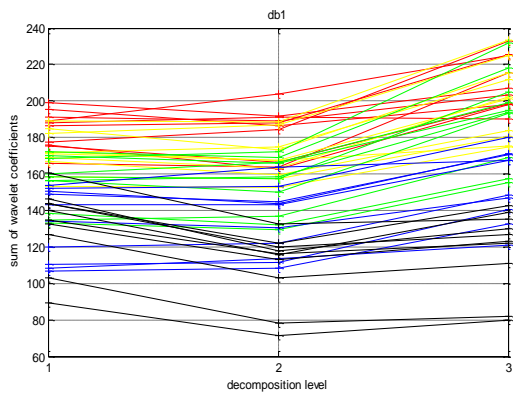


Fig. 8a: Daubechies 1 wavelet decomposition

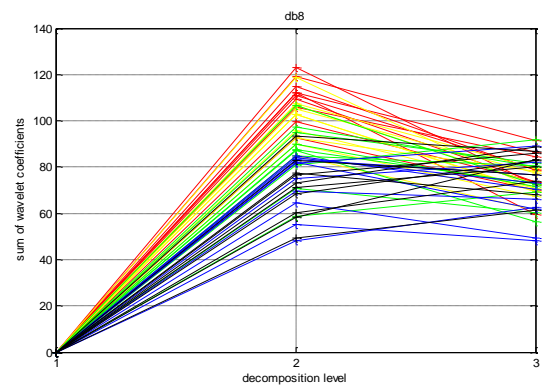


Fig. 8b: Daubechies 8 wavelet decomposition

The first criterion  $K_e$  was derived from Daubechies wavelet function 1. Wavelet coefficients  $c_{i,j}$  form well separated horizontal levels for each class (Fig. 11a). Eq. 2 describes used formula for  $K_e$  evaluation.

$$K_e = \sum_{i=1}^M \sum_{j=1}^N c_{i,j} \quad (2)$$

The other  $K_{s1}$  and  $K_{s2}$  criteria were generated from Daubechies wavelet function 8. Dependence of wavelet coefficients sum on decomposition level has different behaviour for classes with maximum

value at the second level of decomposition (Fig. 11b). This facts lead to design of two criteria from angular coefficient (Eq. 3, 4).

$$K_{s1} = \sum_{i=1}^M \sum_{j=1}^N c_{i,j}^{2^{nd} level} - c_{i,j}^{1^{st} level} \quad (3)$$

$$K_{s2} = \sum_{i=1}^M \sum_{j=1}^N c_{i,j}^{3^{rd} level} - c_{i,j}^{2^{nd} level} \quad (4)$$

Classification criteria were evaluated for image library and intervals for each class were derived using their mean value and standard deviation. According to these values, the classification table was generated (Table 5).

Table 5: CLASSIFICATION TABLE BASED ON WAVELET TRANSFORM

Criterion	Class				
	1	2	3	4	5
$K_e$	> 187,1	(187,1; 171,9)	(171,9; 159,9)	(159,9; 131,0)	131,0 >
$K_{s1}$	> 115,3	(115,3; 97,6)	(97,6; 79,4)	(79,4; 71,9)	79,4 >
$K_{s2}$	> -32,0	(-32,0; -17,7)	(-17,7; -10,4)	(-10,4; 0)	0 >

#### 4 Air Pollution Data Classification

Next part of this project is devoted to application of suggested classification tables to real images coming from various places of the Czech Republic (Fig. 9). More than 400 images were processed and results were compared with their sensual evaluation. Because of elimination of evaluator's mistake, variance  $\pm 1$  class was accepted as a successful result.

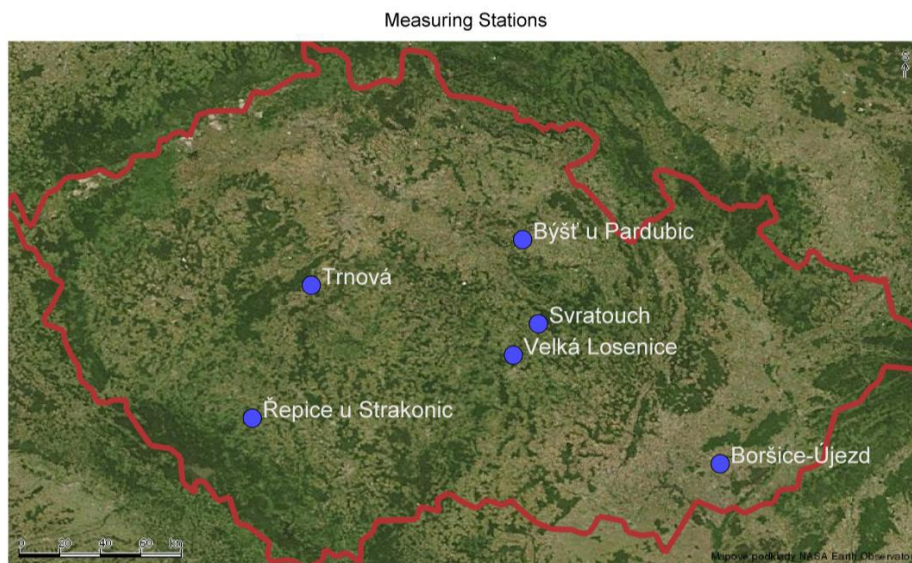


Fig. 9: Map of measuring stations

Images were segmented to  $128 \times 128$  p parts and classified by suggested classification tables after their pre-processing. In the next step, only stoma segments were chosen and their mean values were evaluated. The whole algorithm is presented in Fig. 10 and selected example of its result is shown in Fig. 11, 12.

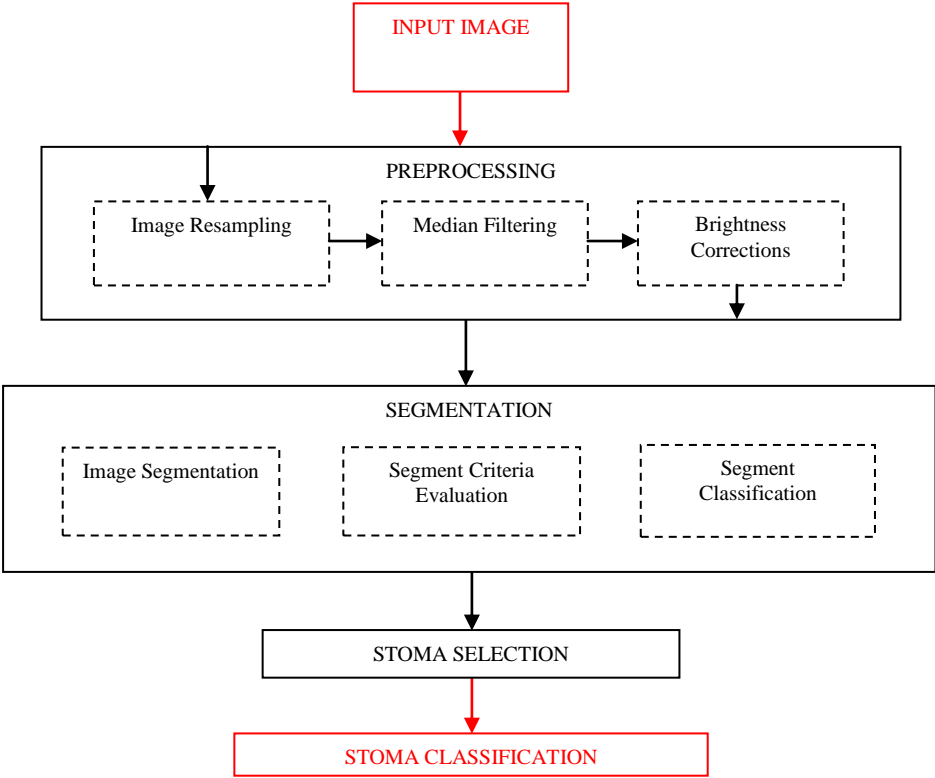


Fig. 10: Classification algorithm

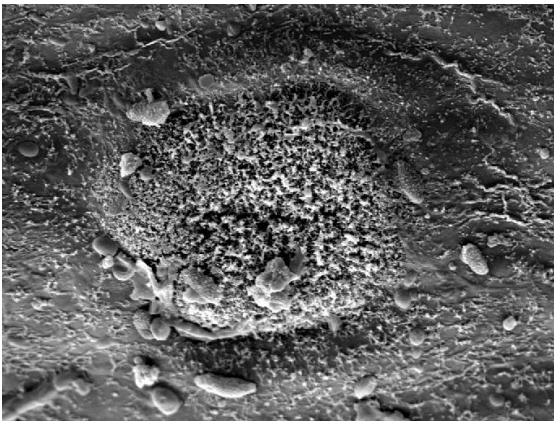


Fig. 11: Original image

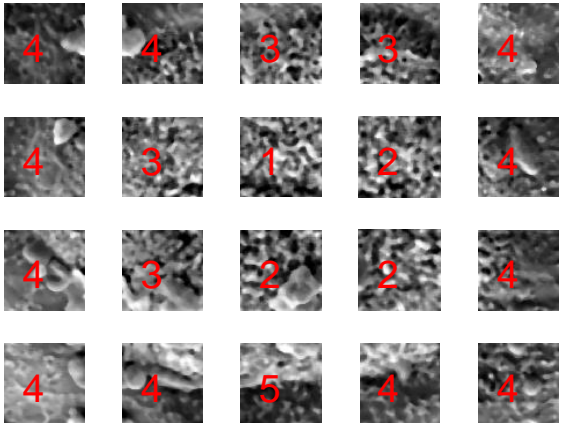


Fig. 12: Classified stoma

## 5 Results and Discussion

Classification tables of all 4 criteria were applied to unknown data. Efficiency of classification is presented in Table 6. Results of algorithmic classification were compared with subjective evaluation.

It is obvious that the best classification was achieved using edge detection criterion  $K_g$ . It agrees with subjective evaluation in 95 per cent. It is possible to obtain sufficient result by means of the first wavelet criterion  $K_{s1}$ , as well.

Table 6: AGREEMENT RATE OF ALGORITHMIC AND SUBJECTIVE IMAGE CLASSIFICATION

Criterion	$K_g$	$K_{s1}$	$K_{s2}$	$K_e$
Classification deviation $\pm 1$ class (%)	95,40	92,33	81,33	87,98
Classification deviation $\pm 2$ class (%)	4,60	6,65	17,90	11,25
Classification deviation $\pm 3$ class (%)	0,00	1,02	0,77	0,77
Average deviation (class)	1,08	1,16	1,27	1,19

## References

- [1] J. Náhlík, P. Cudlín, E. Kašová, R. Bartoničková. *Studium morfológie stomatálného vosku smrku ztepilého na vybraných lokalitách ČR pomocí ERM*. Medzinárodná vedecká konferencia „Stav a Perspektivy ekologického výskumu horských lesných ekosystémov“ – Polana 2001, Sborník přednášek a posterů v plném znění na CD ROM. Slovenská republika, Polana – 22.-25. říjen 2001.
- [2] P. Slavíková, M. Mudrová. *Texture Structure Analysis in Environmental Images*. Humusoft Praha, November 2008. Conference Proceedings, ISBN 978-80-7080-692-0.
- [3] R. C. Gonzalez, R. E. Woods. *Digital Image Processing*. Second edition. Prentice-Hall, New Jersey, USA, 2002. ISBN 0-201-18075-8
- [4] V. Hlaváč, M. Sedláček. *Zpracování obrazů a signálů*. Second Edition. Vydavatelství ČVUT, Praha, 2005. ISBN 80-01-03110-1
- [5] J. Žára, B. Beneš, J. Sochor, P. Felkel. *Moderní počítačová grafika*. Second edition. Computer Press, Brno, 2004. ISBN 80-251-0454-0
- [6] G. Strang, T. Nguyen. *Wavelets and Filter Banks*. Wellesley-Cambridge Press. 1996

---

Petra Slavíková

DCCE ICT Prague, Technická 1905, 166 28 Prague 6, CR, Phone: +420 220 444 027, Fax: +420 220 445 053, E-mail: slavikop@vscht.cz

Martina Mudrová

DCCE ICT Prague, Technická 1905, 166 28 Prague 6, CR, Phone: +420 220 444 027, Fax: +420 220 445 053, E-mail: mudrovam@vscht.cz